COMPUTATIONAL DEM ANALYSIS OF STICK-SLIP DYNAMICS IN THE VERTICAL LUNAR REGOLITH CONVEYOR UNDER EARTH AND LUNAR GRAVITY. L. A. Manolescu[1] and Q. Chen[2], [1]Clemson University, Glenn Department of Civil Engineering, Clemson, SC 29631, lmanole@clemson.edu [2]Clemson University, Glenn Department of Civil Engineering, Clemson, SC 29631, qiushi@clemson.edu

Introduction: The Vertical Lunar Regolith Conveyor (VLRC) is a regolith transport system developed by NASA Kennedy Space Center (KSC) to function on the lunar surface during future In-Situ Resource Utilization (ISRU) efforts [1]. Specifically, the VLRC will serve to transport lunar regolith from the lunar surface into ISRU reactors located on a lander deck similar to Fig. 1.

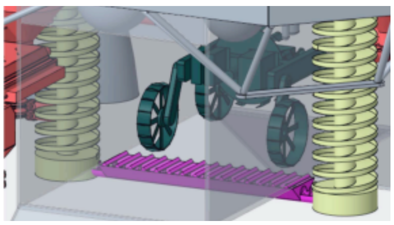

Fig. 1: *Lander deck concept with dual VLRC (yellow)[2]*

The uniqueness of this conveyor lies in its dynamic motion, where it adopts a "stick-slip" repeated 10-degree stroke that gradually moves the regolith upwards along the track of the VLRC [3]. This particular motion was chosen due to its dust tolerance, higher transport efficiency, and lower wear and tear compared to "throwing" conveyors [3]. The stick-slip motion has a prescribed stroke frequency, which determines the acceleration and time duration of the "stick" and "slip" phases.

To maximize self-sustainability on the lunar surface, it is important to maximize efficiency. The purpose of this study is to perform a computational analysis of the influence of stick-slip stroke frequency on regolith mass flow rate in Earth and lunar gravity using Discrete Element Method (DEM) modeling. This was completed using a single loop geometric portion of the VLRC shown in Fig. 2, with the VLRC size corresponding to the VLRC tested in a Low Earth Orbit (LEO) test [4].

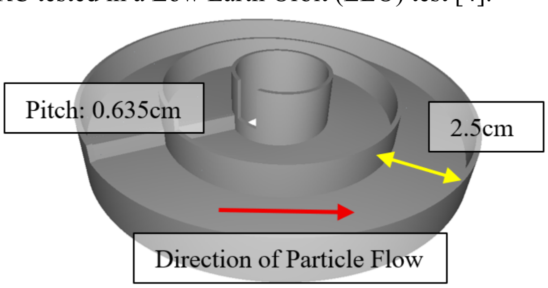

Fig. 2: *Single-loop VLRC geometry used in DEM*

DEM Model Setup: DEM is ideal for modeling regolith as it accurately depicts regolith particle-to-particle interactions and mechanical behaviors. In this study, Altair EDEM is used for all DEM simulations. Lunar regolith particles are represented as a collection of spherical particles that are given physical properties. In the case of the VLRC, the lunar regolith placed into the conveyor was calibrated after Black Point-1 (BP-1), and calibrated parameters are shown in Tab. 1 [5].

Parameter	Value	Unit
Poisson's Ratio	0.25	-
Solids Density	2750	kg/m^3
Shear Modulus	1.00E+07	Pa
(P-P) Resitution Coefficient	0.3	-
(P-P) Static Friction Coefficient	0.85	-
(P-P) Rolling Friction Coefficient	0.8	-
(P-G) Restitution Coefficient	0.3	-
(P-G) Static Friction Coefficient	0.7	-
(P-G) Rolling Friction Coefficient	0.1	-
JKR Surface Energy	0	J/m^2

Tab. 1: *DEM contact model parameters*

Each BP-1 particle was modeled as a double-sphere shape to partially account for the jagged shape of actual regolith particles [5]. Each individual sphere specified a radius of 0.25 mm, and the total sample mass was 5 grams for each trial, equating to a particle count of approximately 15,000 particles. For each test, the sample was generated through a static factory where all particles were generated at once and dropped into the outer track of the VLRC, with the stick-slip motion beginning at 3 seconds. The stick-slip motion was calculated for frequencies ranging from 2.0 Hz to 4.4 Hz per VLRC developer specifications [3]. For each chosen frequency, the angular accelerations and stroke times were found to fit the desired velocity profile shown in Fig. 3.

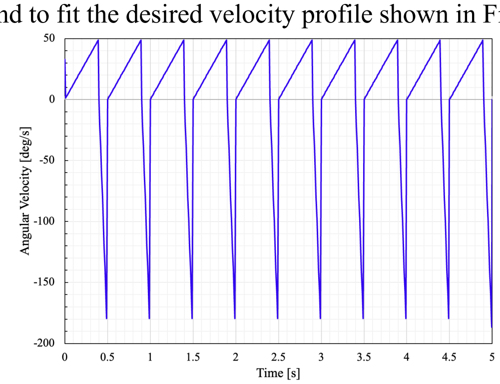

Fig. 3: *Angular velocity profile for stick-slip motion*

To quantify the efficiency of the system, the mass flow rate (MFR) at various points around the VLRC was measured along with a recording of the total accumulated mass at the end of the inclined loop. Each trial was concluded once steady-state was reached. Steady-state was defined as the point at which MFR stabilizes at all sensors.

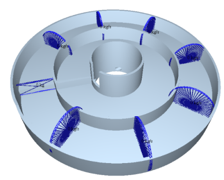

Fig. 4: *MFR sensors (cir.) and accum. mass sensor (rect.)*

Fig. 5: *Lunar regolith transport under 4.4 Hz frequency at: (L) t = 5 s; (M) t = 15 s; (R) t = 90 s (steady-state).*

Mass Flow in Earth and Lunar gravity: Each specified frequency was ran two times in total, once in Earth gravity and once in lunar gravity. At the conclusion of all trials, it was evident that frequency had a direct correlation to reaching steady-state for Earth gravity, with a significantly improved time to steady-state for frequencies 4.0 Hz and above. A sample plot of the 4.4 Hz trial is given in Fig. 6 and Fig. 7. Lunar gravity observed a similar MFR trend with steady-state being reached sooner with increasing frequency, but with 2.0 Hz as an outlier, reaching steady state prior to 2.5 Hz.

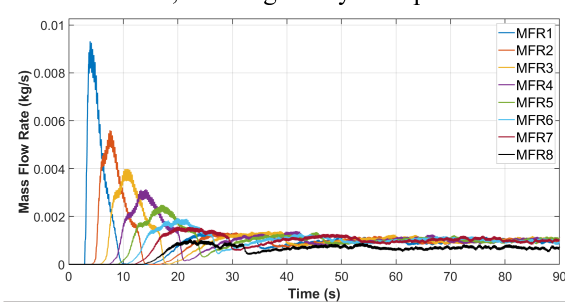

Fig. 6: *MFR over time for 4.4 Hz Earth gravity trial*

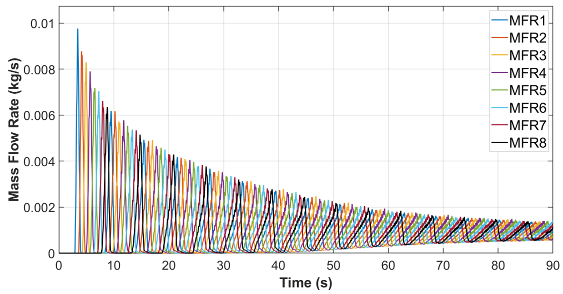

Fig. 7: *MFR over time for 4.4 Hz lunar gravity trial*

As for total mass accumulation, an increase in frequency resulted in a faster mass accumulation in all Earth gravity trials, except for an outlier in 3.5 Hz. A significant increase in efficiency for Earth gravity can be noted at 4.0 Hz, as the sample is able to fully complete the VLRC loop. In lunar gravity trials, a significant jump in efficiency occurred from 2.0 Hz to 2.5 Hz; but these efficiency gains decrease dramatically in the 3.0 Hz to 4.4 Hz range.

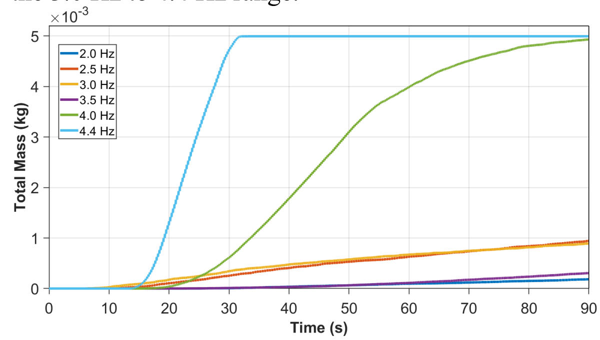

Fig. 8: *Accumulated mass vs time for all Earth gravity trials*

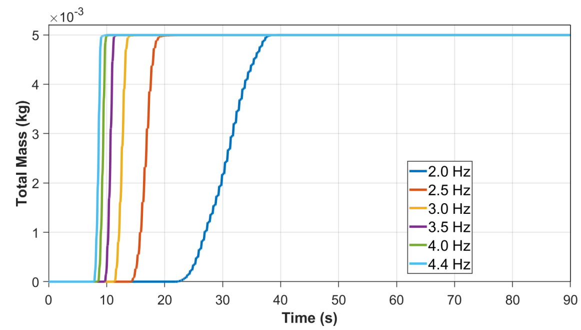

Fig. 9: *Accumulated mass vs time for all lunar gravity trials*

Summary: This study used DEM simulations to evaluate VLRC performance under varying gravity and frequencies. Results show that stroke frequency directly dictates mass flow and efficiency. In Earth gravity, frequencies of 4.0 Hz or higher are essential for the regolith to complete the loop and reach steady-state. Conversely, lunar trials reached steady-state faster, showing a major efficiency surge between 2.0 Hz and 2.5 Hz, followed by diminishing returns at higher frequencies. These findings shed light on optimizing "stick-slip" mechanics to ensure reliable regolith transport for future ISRU missions.

References: [1] Mantovani J. G. et al. (2023) *Space Resources Roundtable XXIII*, Abstract #20230008564. [2] Linne D. L. et al. (2021) *J. Aerosp. Eng., 34*, 0402143. [3] Olson A. et al. (2022) *Space Resources Roundtable XXII*. [4] Mantovani J. G. et al. (2025) *VLRC Suborbital Flight Payload Overview*. [5] Gaines D. et al. (2024) *Earth and Space*, 356–365.

Acknowledgment: This research is partially supported by NASA under the federal awards No. 80NSCC20M0054 (sub-award 20-013-REAP-CU015) and 80NSSC25M7077 (sub-award No. 25-073-GRF-CU-005). The results and opinions expressed in this paper do not necessarily reflect the views and policies of NASA.